buildings

MDPI

Article

A COMSOL–MATLAB Coupled Optimization Framework for Cost-Effective Acoustic Renovation of Educational Buildings Using Wood-Based Materials

Shuang Yan [1], Liutao Zhang [1,*], Zhenbo Liu [2,*] and Yuanyuan Miao [2]

[1] Jiyang College, Zhejiang Agriculture and Forestry University, Zhuji 311800, China
[2] College of Materials Science and Engineering, Northeast Forestry University, Harbin 150040, China
* Correspondence: 20199037@zjyc.edu.cn (L.Z.); liu.zhenbo@nefu.edu.cn (Z.L.)

Abstract

Poor classroom acoustic conditions can impair speech intelligibility, increase cognitive load, and reduce the quality of learning environments. Simulation-guided optimization provides a promising approach for improving building acoustic performance and indoor environmental quality while reducing trial-and-error material selection in renovation practice. The field-validated optimized configuration combined slotted wood sound-absorbing panels and mineral wool panels, with a total material cost of 1512 RMB. Field measurements showed that this configuration reduced RT from 2.42–1.76 s to 0.78–0.43 s. In addition, the simulation-based STI evaluation increased from 0.19 to 0.75, indicating a potential improvement in speech intelligibility. Since STI was not directly measured in the field, this result is interpreted as a model-based prediction supported by the calibrated RT validation. The average relative error between simulated and measured RT values was 6.83%, demonstrating the predictive reliability of the calibrated model for RT prediction. The proposed framework provides a practical decision-support method for cost-controlled acoustic renovation of educational buildings and was validated using an existing classroom case. The framework was demonstrated using one existing classroom and provides a methodological basis for adaptation to other educational spaces by updating room-specific inputs. Its external transferability requires validation in additional classrooms.

Keywords: educational buildings; wood-based acoustic materials; reverberation time; speech transmission index

Check for updates

Academic Editor: Francesco Nocera

Received: 28 May 2026
Revised: 17 June 2026
Accepted: 2 July 2026
Published: 6 July 2026

Copyright: © 2026 by the authors. Licensee MDPI, Basel, Switzerland. This article is an open access article distributed under the terms and conditions of the Creative Commons Attribution (CC BY) license.

1. Introduction

Classroom acoustic conditions strongly influence learning performance, acoustic comfort, and speech intelligibility [1–5]. However, many existing classrooms still suffer from excessive background noise, long RT, and uneven sound transmission, which can cause speech distortion, reduced audibility, and increased cognitive load [6–9]. RT and STI are commonly used to evaluate classroom acoustic quality and speech intelligibility [10–15]. Because room geometry, furniture layout, and surface materials determine sound propagation and reflection patterns, acoustic renovation usually depends on the rational selection and placement of sound-absorbing materials [16–19].

Material selection is a key factor influencing classroom acoustic performance. Hard surfaces such as concrete and glass reflect sound strongly, increasing RT and reducing speech clarity [20]. Wood and wood-based acoustic materials have been widely investigated for indoor acoustic regulation because their porous structures, surface textures, and

processable geometries can regulate sound absorption, reflection, and diffusion [21–24]. As renewable interior products with potential environmental advantages, they are compatible with educational spaces and can improve classroom RT and speech transmission quality when properly configured [25–28]. Previous studies have shown that acoustic renovation using green materials, fiberglass panels, curtains, and wall–ceiling absorptive treatments can effectively reduce classroom RT and improve speech intelligibility [29–32]. Numerical tools such as Ecotect, COMSOL Multiphysics, and CadnaR have also been used to evaluate classroom acoustic performance and guide material placement [30–32]. Other studies have examined the influence of absorptive material placement on walls, ceilings, and reflective areas [33–35]. These studies demonstrate that acoustic material selection and spatial placement are effective strategies for improving classroom acoustic quality. In addition to acoustic performance, renovation cost is an important factor affecting the feasibility of acoustic treatment in existing educational buildings. Therefore, this study incorporates material cost as an explicit optimization objective rather than treating it only as a post-design consideration.

Although Building Performance Optimization studies have increasingly incorporated multiple objectives, cost considerations in acoustic renovation research are frequently addressed as post-design assessments rather than integrated optimization targets during early-stage decision-making. In addition, most existing studies focus on material performance comparison, empirical layout adjustment, or simulation-based evaluation after a design scheme has already been proposed. Therefore, there remains a lack of transparent decision-support frameworks capable of simultaneously optimizing acoustic performance, material layout, and renovation cost under practical constraints.

To address this gap, this study develops and validates a COMSOL–MATLAB coupled simulation–optimization framework for cost-effective acoustic renovation of educational buildings. The framework links acoustic prediction, evolutionary material-layout optimization, cost constraints, constructability considerations, and field validation, thereby providing a modular decision-support workflow with the potential for adaptation to other educational buildings. The contributions of this study are fourfold. First, a COMSOL–MATLAB coupled simulation–optimization workflow was developed to connect room-acoustic prediction with evolutionary material-layout optimization for acoustic renovation of educational buildings, using a real classroom as the validation case. Second, the framework integrates RT, STI, material cost, installation area, and constructability constraints, thereby transforming acoustic material selection from an experience-based process into a quantitative building performance optimization problem for renovation practice. Third, the optimized configuration was implemented in a real classroom and validated through field RT measurements to examine the predictive reliability of the calibrated acoustic model for RT prediction. Fourth, the acoustic improvement mechanism was interpreted from the perspectives of resonance absorption, porous dissipation, frequency-band complementarity, and spatial material synergy, providing design implications for cost-effective acoustic renovation of educational buildings.

2. Materials and Methods

2.1. Acoustic Quality Index

2.1.1. Reverberation Time

Reverberation time (RT) was used to evaluate the acoustic decay characteristics of the classroom. In this study, RT was calculated based on the room volume, total surface area, air attenuation coefficient, and average sound absorption coefficient, as expressed in by the following formula. The RT value depends on the average sound absorption coefficient

$\overline{\alpha}$, which was calculated from the sound absorption coefficients of the selected acoustic materials at 250, 500, 630, 800, 1000, and 2000 Hz.

$$T_{60,E} = \frac{0.161V}{-SIn(1-\overline{\alpha}) + 4\,mV}$$

where $T_{60,E}$ is the RT, where the sound is reduced by 60 dB in the unit of s; V is the volume of the room, S is the total surface area of the room; m is the attenuation coefficient of sound in the air; $\overline{\alpha}$ is the average indoor sound absorption coefficient.

2.1.2. Speech Transmission Index

Speech intelligibility was evaluated using the speech transmission index (STI), which was used as the primary speech-clarity indicator in the optimization constraints and result evaluation [36]. To further interpret the influence of reverberation on speech perception, the percentage articulation loss of consonants (%ALCons) was introduced as a supplementary explanatory indicator [37–39]. In this study, STI was used for optimization and compliance assessment, whereas %ALCons was used only to explain the relationship between RT and speech clarity.

$$Alcons \approx 0.652\left(\frac{r_{LH}}{r_H}\right)^2 RT\%$$

where r_{LH} is the distance between the sound source and the listener, r_H is the reverberation radius. Ideal clarity $\leq$ 3%, good clarity 3–8%, satisfactory clarity 8–11%, poor clarity > 11%, worthless clarity > 20% (limit value 15%). A longer RT generally results in greater articulation loss and reduced speech clarity [37–39].

2.2. Materials

The wood-based sound-absorbing materials included slotted wood sound-absorbing panels, perforated wood sound-absorbing panels, and wood wool sound-absorbing panels. The other acoustic materials included polyester fiber acoustic panels, fabric-covered acoustic panels, perforated calcium silicate panels, perforated composite gypsum panels, PVC acoustic panels, and mineral wool panels. Their dimensions and structural parameters are listed in Table 1 and Figure 1. All candidate acoustic and interior finishing materials were supplied by Hangzhou Geli Building Materials Technology Co., Ltd. (Hangzhou, China).

Table 1. Dimensions and structural parameters of the acoustic material specimens.

Category	Material	Length (mm)	Width (mm)	Thickness (mm)	Aperture (mm)	Hole Center Distance (mm)	Slot Width (mm)
Wood-based sound-absorbing material	Slotted wood sound-absorbing panel	2440	197	15	8	15, 17	3
	Perforated wood sound-absorbing panel	2440	197	12	32	8	/
	Wood wool sound-absorbing panel	2420	1220	9	/	/	/
Other sound-absorbing materials	Polyester fiber acoustic panel	2420	1220	9	/	/	/
	Fabric-covered acoustic panel	1200	600	15	/	/	/
	Perforated calcium silicate panel	1200	600	6	8	20	/
	Perforated composite gypsum panel	600	600	20	8	16	/
	PVC acoustic panel	2440	197	15	/	/	/
	Mineral wool panel	3000	210	12	/	/	/

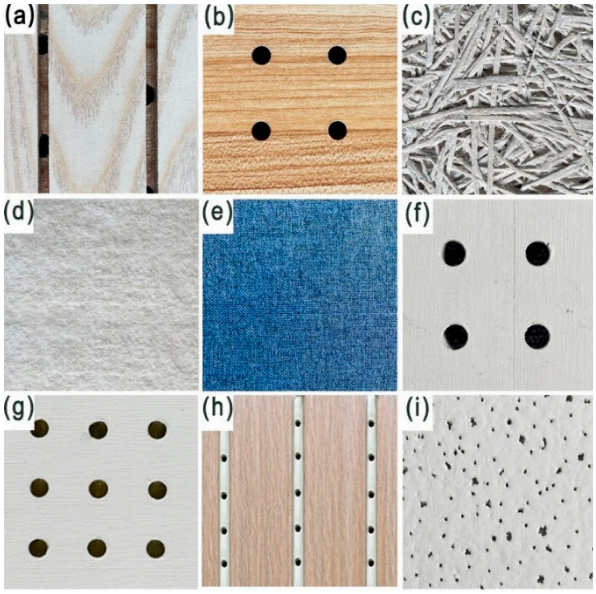


Figure 1. Candidate acoustic materials used in this study: (**a**) slotted wood sound-absorbing panel; (**b**) perforated wood sound-absorbing panel; (**c**) wood wool sound-absorbing panel; (**d**) polyester fiber acoustic panel; (**e**) fabric-covered acoustic panel; (**f**) perforated calcium silicate panel; (**g**) perforated composite gypsum panel; (**h**) PVC acoustic panel; and (**i**) mineral wool panel.

The sound absorption coefficients were measured according to GBJ 88-1985 and GB/T 18696.1-2004 [40,41] using the standing-wave tube method with an impedance tube system (AWA6122 intelligent electroacoustic tester, Aihua, Hangzhou, China; tube diameter: 92 ± 1 mm). For each material, six specimens were tested, and the mean absorption coefficient was calculated for each frequency band. Because classroom acoustic evaluation commonly emphasizes the 500–2000 Hz frequency range according to GB 50118-2010 [42], the measured absorption coefficients across the tested frequency bands were used as material inputs for the acoustic simulation. The measured sound absorption coefficients are listed in Table 2.

Table 2. Frequency-dependent sound absorption coefficients of candidate acoustic materials.

Material Category	Material	Absorption Coefficient					
		250 Hz	500 Hz	630 Hz	800 Hz	1000 Hz	2000 Hz
Wood-based sound-absorbing material	Slotted wood sound-absorbing panel	0.77	0.98	0.99	0.99	0.81	0.52
	Perforated wood sound-absorbing panel	0.91	0.74	0.67	0.65	0.54	0.46
	Wood wool sound-absorbing panel	0.83	0.99	0.95	0.96	0.97	0.83
Other sound-absorbing materials	Polyester fiber acoustic panel	0.58	0.97	0.96	0.98	0.98	0.97
	Fabric-covered acoustic panel	0.55	0.82	0.81	0.71	0.72	0.69
	Perforated calcium silicate panel	0.74	0.94	0.96	0.99	0.82	0.55
	Perforated composite gypsum panel	0.80	0.79	0.65	0.60	0.47	0.30
	PVC acoustic panel	0.55	0.74	0.68	0.58	0.74	0.46
	Mineral wool panel	0.38	0.30	0.52	0.84	0.78	0.72

2.3. Methods

The proposed workflow consists of five steps: (i) measuring the acoustic properties of candidate materials; (ii) constructing and calibrating a classroom acoustic model in COMSOL; (iii) defining decision variables, constraints, and objective functions in MATLAB; (iv) optimizing material type, coverage area, and installation location using a genetic

algorithm; and (v) validating the optimized scheme through field measurements in a real classroom. Acoustic formulas were used to quantify the acoustic performance requirements and support the definition of optimization constraints [43].

3. Optimization Model Formulation

The optimization model was formulated by defining the classroom acoustic parameters, design variables, material-layout constraints, acoustic performance constraints, and objective function.

3.1. Classroom Geometry and Acoustic Model

The classroom was measured on site according to GB/T 36075.2-2018 [44] to obtain acoustic parameters for model calibration. A representative rectangular classroom was selected as the case study, with an indoor temperature of 20 °C and relative humidity of 50% during measurement. The classroom was 8.86 m long, 8.00 m wide, and 3.75 m high. It contained two doors, five glass windows, 20 desks, 40 chairs, and a podium. The walls were finished with painted concrete, while the desks and chairs were made of PVC. The RT of the classroom was measured, and an omnidirectional sound source was placed directly in front of the podium to simulate the position of the teacher in class. Six representative receiver points (M1–M6) were selected in the student seating area. The receiver height was 1.2 m above the floor. Pink noise was used as the excitation signal and reproduced by an AE2001 dodecahedral loudspeaker through a power amplifier. The acoustic responses at the receiver positions were recorded using a BSW801 system and an XM802 handheld acoustic analyzer. The impulse responses and sound-field parameters were then calculated from the recorded signals.

A three-dimensional classroom model was constructed using CAD and Rhinoceros and then imported into COMSOL Multiphysics for acoustic ray-tracing simulation. The total volume was 265.8 m^3, and the total surface area was 291.27 m^2. To simplify the model, the desk and seating area were represented as a rectangular volume with a height of 0.75 m. The seating area was modeled without occupants. The sound-source and receiver positions in the simulation were kept consistent with those used in the field measurements. The surface materials in the classroom were assigned frequency-dependent sound absorption coefficients, as listed in Table 3 [43]. The number of emitted acoustic rays was set to 6000. The ray-acoustics simulation was performed using frequency-dependent boundary absorption coefficients for the classroom surfaces and candidate acoustic materials. The omnidirectional sound-source and receiver positions were kept consistent with the field measurement setup. Air attenuation was considered under the measured indoor environmental conditions of 20 °C and 50% relative humidity. The acoustic model was calibrated using the measured classroom data because scattering coefficients strongly affect the accuracy of room-acoustic simulations [45–47]. The scattering coefficients of major interior surfaces were initially assigned according to values reported in previous room-acoustic simulation and classroom RT prediction studies [45–48]. Iterative adjustments were subsequently performed to minimize the average relative error between the simulated and measured RT values across the six investigated frequency bands, namely 250, 500, 630, 800, 1000, and 2000 Hz. The final calibrated coefficients were 0.6 for desks and chairs, and 0.05 for flat surfaces, resulting in an average relative error of 6.83% between simulated and measured RT values.

Table 3. Sound absorption coefficients of classroom surface materials [43].

Position	Material	250 Hz	500 Hz	630 Hz	800 Hz	1000 Hz	2000 Hz
Wall surface	Concrete paint	0.1	0.05	0.06	0.07	0.09	0.08
Door	Honeycomb panel	0.01	0.01	0.02	0.02	0.02	0.02
Window	Glass (thickness 0.3 cm)	0.35	0.25	0.18	0.12	0.07	0.04
Floor	Tiles	0.01	0.01	0.02	0.02	0.02	0.02
Seats	PVC	0.02	0.01	0.01	0.02	0.03	0.04

3.2. Decision Variables

Location variables. Because both side walls contain windows, they were excluded from acoustic material installation. The front wall, ceiling, and rear wall were therefore selected as candidate treatment surfaces. The installation positions on the front wall, ceiling, and rear wall were represented by coordinate variables in MATLAB. These variables defined the panel locations within the available surface boundaries.

Coverage-area variables. The coverage area of each acoustic treatment was determined by length and width variables, while material thickness was assigned according to the selected material type. The front wall was represented by xce, yce, and thce; the ceiling by xt, yt, and thtop; and the rear wall by xback, yback, and thback.

Material-type variables: material types were encoded as discrete integer variables and selected from the candidate material database according to their sound absorption coefficients and feasible installation locations.

The complete set of decision variables, including installation position, coverage area, material thickness, and material category for the front wall, ceiling, and rear wall, is summarized in Table 4.

Table 4. Decision variables for material type, installation position, and coverage area in the optimization model.

Treatment Surface	Position Variables	Coverage-Area Variables	Thickness Variable	Wood-Based Material Variable	Other Acoustic Material Variable
Front wall	$x_{ce,axis}$, $y_{ce,axis}$	x_{ce}, y_{ce}	th_{ce}	w_{ce}	o_{ce}
Ceiling	$x_{t,axis}$, $y_{t,axis}$	x_t, y_t	th_{top}	w_{top}	o_{top}
Rear wall	$x_{back,axis}$, $y_{back,axis}$	x_{back}, y_{back}	th_{back}	w_{back}	o_{back}

In Table 4, the position variables define the starting coordinates of the installed acoustic treatment on each candidate surface. The coverage-area variables determine the length and width of the installed material area, while the thickness variables are assigned according to the selected material type. The variables w and o represent the selected wood-based sound-absorbing material and other acoustic material categories, respectively. These variables were used in MATLAB to generate candidate material-layout solutions for COMSOL acoustic simulation.

3.3. Acoustic and Material Constraints

3.3.1. Acoustic Performance Constraints

The acoustic performance constraints were defined according to the target RT and STI values required for classroom speech intelligibility. For each receiver position, RT was constrained to be no greater than 1.0 s, while STI was constrained to be no less than 0.60. These thresholds ensured that the optimized classroom satisfied both reverberation control and speech intelligibility requirements.

3.3.2. Material Layout Constraints

The material layout constraints were introduced to ensure that the selected acoustic materials could be installed within the available surface areas of the classroom. The coverage area of acoustic materials on the front wall, ceiling, and rear wall was constrained by the corresponding surface dimensions. Lower and upper bounds were assigned to the coordinate, length, and width variables to prevent candidate panels from exceeding the available installation regions.

3.3.3. Material Selection Constraints

The material selection constraints were introduced to ensure practical constructability and design feasibility. Candidate materials were selected from the material database listed in Table 5. For each installation surface, only one acoustic material was allowed to be assigned in order to simplify construction and maintain visual consistency. The selected material type had to satisfy the feasible installation location specified in the material database. Candidate acoustic materials and their unit prices used in the optimization model are listed in Table 5.

Table 5. Candidate acoustic materials and unit prices used in the optimization model.

Material Category	Material	Use Location	Price (RMB/m^2)
Wood-based sound-absorbing material	Slotted wood sound-absorbing panel	Wall and ceiling	32
	Perforated wood sound-absorbing panel	Wall and ceiling	58
	Wood wool sound-absorbing panel	Wall and ceiling	29.7
Other sound-absorbing materials	Polyester fiber acoustic panel	Wall and ceiling	24
	Fabric-covered acoustic panel	Wall facing	72
	Perforated calcium silicate panel	Wall and ceiling	29
	Perforated composite gypsum panel	Wall and ceiling	27
	PVC acoustic panel	Wall and ceiling	80
	Mineral wool panel	Wall and ceiling	16

3.4. Objective Function

The optimization objective was to minimize the total material cost, while RT and STI were treated as acoustic performance constraints. In this study, the cost model focused on material cost rather than full life-cycle cost. This simplification was adopted because material unit prices and coverage areas can be clearly defined and consistently integrated into the optimization model, whereas installation, maintenance, replacement, and life-cycle costs may vary substantially depending on local labor prices, construction methods, contractor practices, and long-term facility-management conditions. Therefore, the present model should be interpreted as a material-cost optimization model for early-stage acoustic renovation decision support. This formulation reflects practical renovation scenarios in which the acoustic targets must first be satisfied, and the material cost is then minimized among feasible solutions. The total material cost was calculated as:

$$C = \sum_{j=1}^{n} p_j A_j$$

where C is the total material cost, p_j is the unit price of material j, A_j is the selected coverage area of material j, and n is the number of selected acoustic materials.

3.5. GA-Based COMSOL–MATLAB Optimization Procedure

The optimization model was implemented using a genetic algorithm (GA) in MATLAB 2021b [49] and coupled with the COMSOL acoustic model. A mixed-variable encoding strategy was adopted. Continuous variables were used to represent panel position and coverage area on the front wall, ceiling, and rear wall, whereas discrete integer variables were used to represent material types.

In the coupled workflow, MATLAB first generated a candidate material-layout vector containing material type, installation location, and coverage area. This vector was then transferred to the COMSOL acoustic model to update the boundary absorption conditions and material layout. COMSOL calculated the corresponding RT and STI values at the receiver positions and returned the results to MATLAB for objective-function evaluation and constraint checking. Based on the penalized fitness value, the GA operators, including selection, crossover, and mutation, were applied to generate the next population. This iterative process was repeated until the termination criteria were satisfied.

The fitness function was formulated to minimize the total material cost while satisfying the acoustic performance constraints. To handle infeasible solutions, a penalty term was added to the objective function when a candidate solution failed to satisfy the RT or STI constraints. The penalized fitness function was expressed as:

$$F = C + \lambda \sum_{i} [\max(0, RT_i - 1.0) + \max(0,\ 0.60 - STI_i)]$$

where F is the penalized fitness value, C is the total material cost, λ is the penalty coefficient, and i denotes the receiver position. The term $\max(0, RT_i - 1.0)$ penalizes solutions with excessive RT, whereas $\max(0,\ 0.60 - STI_i)$ penalizes solutions with insufficient speech intelligibility. Because the GA minimized the penalized fitness value, infeasible material configurations received larger penalty values and were therefore less likely to be retained during the evolutionary process.

The GA parameters were set as follows: population size of 200, maximum number of generations of 50,000, crossover rate of 0.8, mutation rate of 0.2, and function tolerance of 10^{-6}. The best feasible objective value in each generation was recorded to monitor convergence. The final feasible solution was selected only when all RT and STI constraints were satisfied and was subsequently evaluated through field validation. The optimization was performed on a laptop equipped with a 12th Gen Intel(R) Core(TM) i9-12900H 2.50 GHz processor (Intel Corporation, Santa Clara, CA, USA), and the total computation time was approximately 170 h. Because the GA is inherently stochastic, three independent optimization runs were conducted using different random initial populations. The population size of 200, maximum number of generations of 50,000, crossover rate of 0.8, mutation rate of 0.2, objective function, candidate material database, acoustic constraints, constructability constraints, and COMSOL classroom model were kept identical across the three runs. The best feasible objective value in each generation was recorded to evaluate convergence behavior and repeatability. A solution was regarded as feasible only when the RT values satisfied the upper limit of 1.0 s and the predicted STI satisfied the lower limit of 0.60. GA was selected because the present optimization problem involves mixed decision variables, including discrete material-type variables and continuous installation-position and coverage-area variables. Moreover, the objective function was evaluated through COMSOL acoustic simulation, making the problem nonlinear, non-smooth, and difficult to solve using gradient-based methods. GA can handle constrained and mixed-variable search spaces without requiring gradient information, which makes it suitable for simulation-based acoustic material-layout optimization. Nevertheless, GA also has limitations. Its results may be affected by random initial populations and algorithm parameters, and the computational cost can be high when

each candidate solution requires COMSOL simulation. Other algorithms, such as particle swarm optimization, simulated annealing, and multi-objective evolutionary algorithms, may also be applicable to this problem. A systematic comparison of these algorithms will be conducted in future work.

3.6. Field Validation Procedure

To evaluate the applicability of the proposed decision model, the optimized acoustic renovation scheme was implemented and measured in an existing classroom. The installation layout used in the field measurement was consistent with the optimized configuration defined in the COMSOL acoustic simulation. Field validation was conducted to verify whether the optimized material configuration could satisfy the RT requirement in the real classroom while maintaining a low material cost. STI was used as a simulation-based speech-intelligibility indicator in the optimization and performance evaluation. Field validation focused on RT measurements because the available field measurement campaign was designed to verify the acoustic decay characteristics of the renovated classroom. Direct STI measurement was not conducted because it requires a more specific speech-transmission measurement setup, including calibrated speech-like test signals, strict background-noise control, and standardized source–receiver measurement procedures. Therefore, STI results in this study should be interpreted as simulation-based predictions rather than direct field measurements. The same sound-source position and six receiver positions used in the baseline measurement and COMSOL simulation were adopted after renovation. RT values were measured at 250, 500, 630, 800, 1000, and 2000 Hz, and the measured results were compared with the simulated values to evaluate model accuracy. The absolute and relative errors between simulated and measured RT values were calculated for each frequency band.

4. Results and Discussion

4.1. Baseline Acoustic Conditions of the Untreated Classroom

Before acoustic renovation, six receiver positions (M1–M6) were selected in the seating area. As shown in Figure 2, the measured RT ranged from 2.42 s to 1.76 s, with particularly long low-frequency reverberation exceeding 2.4 s. The simulation-based STI value of the untreated classroom was 0.19, which did not meet the requirement for acceptable speech intelligibility. The long RT caused sound overlap and reduced speech clarity, while the low STI indicated poor speech-transmission quality in the classroom.

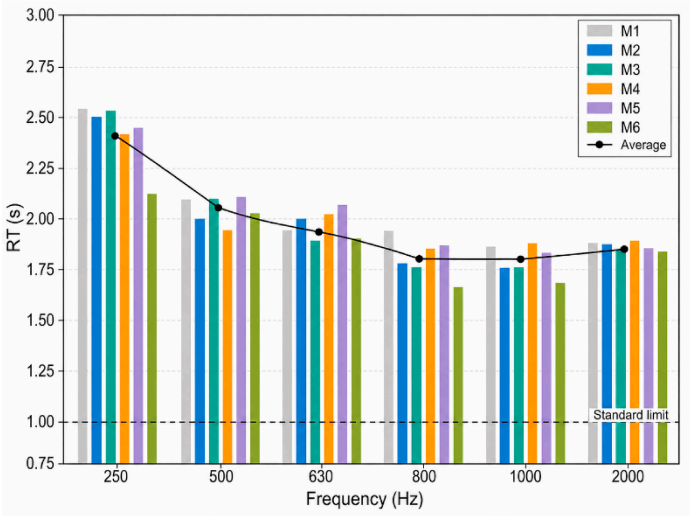


Figure 2. RT values at different receiver positions in the untreated classroom (M1–M6).

Figure 3 shows the simulated sound-energy distribution at 10 ms and 20 ms after sound emission. At 10 ms, acoustic energy was concentrated near the sound source. At 20 ms, sound energy had propagated throughout the classroom, while multiple reflections remained evident. This delayed energy decay explains the long RT and poor STI observed in the untreated classroom.

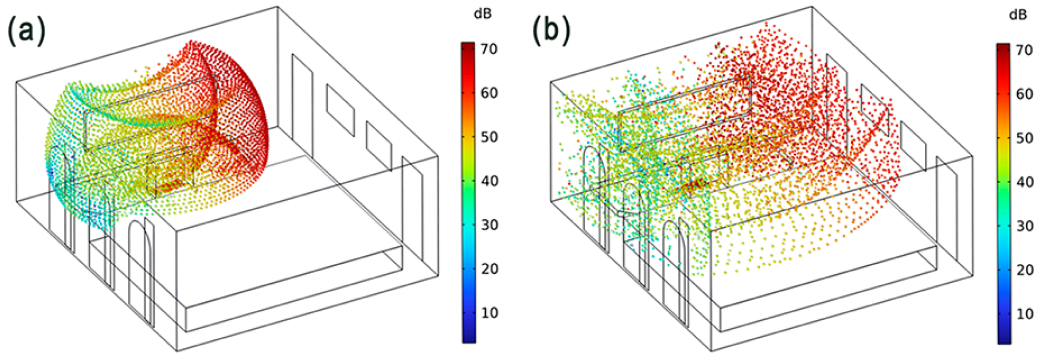


Figure 3. Simulated acoustic ray distribution and sound pressure level from the omnidirectional sound source after (**a**) 10 ms and (**b**) 20 ms.

4.2. GA Optimization Process and Convergence Behavior

A GA-based optimization model was developed to identify material types, coverage areas, and installation locations that reduce RT and improve STI under cost and constructability constraints. The optimization process integrated acoustic simulation results from COMSOL with objective-function evaluation and evolutionary operations in MATLAB.

Figure 4 presents the COMSOL–MATLAB coupled GA optimization framework. In this framework, MATLAB generated candidate material-layout solutions, while COMSOL calculated the corresponding RT and STI values. The acoustic indicators were then returned to MATLAB for objective-function evaluation, constraint checking, and evolutionary operations.

The convergence curve of the reported optimization run is shown in Figure 5, whereas the repeatability of the optimization framework was evaluated through three independent runs summarized in Table 6. Although the three runs showed slightly different convergence rates because of their different random initial populations, all runs gradually converged to similar feasible material-cost solutions under the specified RT and STI constraints. The best feasible objective value decreased rapidly in the early generations and gradually stabilized as the number of generations increased, indicating that the reported optimization run converged to a feasible low-cost solution under the specified RT and STI constraints. The final optimized configuration was further evaluated through field measurements to verify its practical acoustic performance.

To evaluate the robustness and repeatability of the GA-based optimization, three independent runs were conducted using different random initial populations under identical algorithm parameters and constraints. All three runs selected the same material combination of slotted wood sound-absorbing panels and mineral wool panels. In Run 1, the final material cost was 1512 RMB, the predicted RT range was 0.43–0.82 s, the predicted STI was 0.75, and the objective value became stable after approximately 30,000 generations. In Run 2, the final material cost was 1520 RMB, the predicted RT range was 0.44–0.84 s, the predicted STI was 0.74, and convergence occurred after approximately 32,600 generations. In Run 3, the final material cost was 1504 RMB, the predicted RT range was 0.42–0.81 s, the predicted STI was 0.75, and convergence occurred after approximately 28,700 generations.

The same material combination was obtained in all three independent runs. The final material cost ranged from 1504 to 1520 RMB, with a mean value of 1512 RMB, a standard

deviation of 8 RMB, and a coefficient of variation of 0.53%. The predicted STI values varied only between 0.74 and 0.75, and all predicted RT values remained below the 1.0 s limit. These results indicate limited variation across the three runs under the fixed GA parameter settings examined in this study.

The field-validated configuration corresponded to Run 1, with a material cost of 1512 RMB. Runs 2 and 3 were subsequently conducted as repeatability checks and were not implemented in the classroom. Although Run 3 produced a slightly lower simulated material cost of 1504 RMB, the 1512 RMB configuration is reported as the field-validated case rather than as the absolute minimum obtained across all repeated runs.

Although the three independent runs produced similar feasible solutions under the fixed GA parameters, these runs assessed repeatability with respect to different random initial populations only. The population size, crossover rate, mutation rate, and generation limit were kept unchanged across the three runs. Therefore, the results do not constitute a sensitivity analysis of the GA parameter settings. A systematic parameter-sensitivity analysis is still required to determine how these parameters affect convergence efficiency, solution variability, and computational cost.

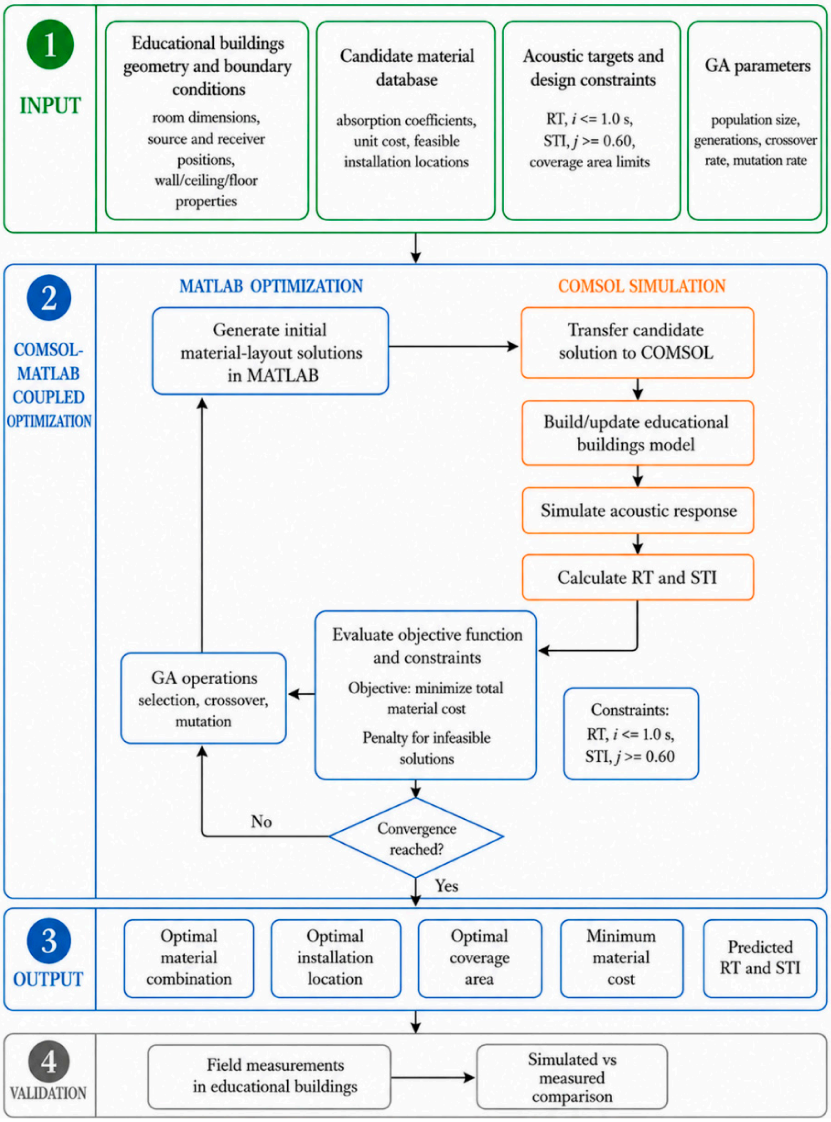


Figure 4. COMSOL–MATLAB coupled simulation–optimization workflow for cost-effective acoustic renovation of educational buildings, including material database construction, acoustic simulation, GA-based optimization, and field validation.

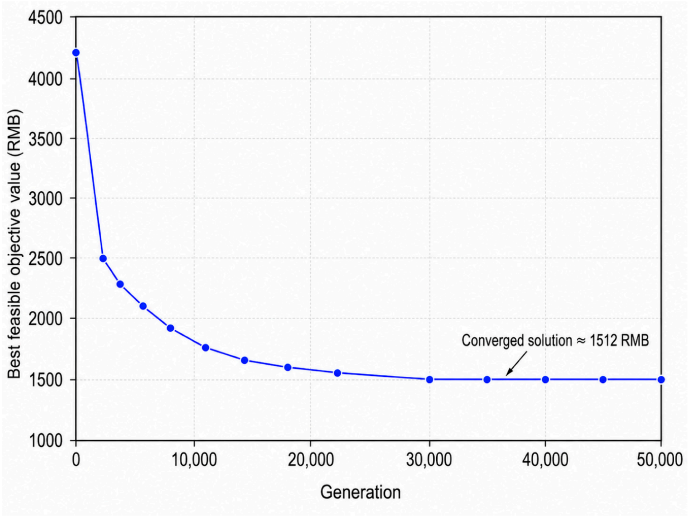


Figure 5. Convergence curve of the GA during material configuration optimization.

Table 6. Repeatability of the GA optimization results under three independent runs.

Parameter	Run 1	Run 2	Run 3
Final material combination	Slotted wood + mineral wool	Slotted wood + mineral wool	Slotted wood + mineral wool
Total material cost (RMB)	1512	1520	1504
Predicted RT range (s)	0.43–0.82	0.44–0.84	0.42–0.81
Predicted STI	0.75	0.74	0.75
Approximate convergence generation	30,000	32,600	28,700

Note: The same material combination was obtained in all three independent runs, while only minor variations were observed in material cost and acoustic predictions. This suggests that the GA-based optimization framework exhibits acceptable robustness against different random initial populations.

Uncertainty in the proposed optimization framework arises from four main sources. First, algorithmic uncertainty is introduced by the random initial population and the stochastic selection, crossover, and mutation operations of the GA. The same material combination was obtained in all three independent runs, and the coefficient of variation in material cost was 0.53%, indicating limited sensitivity to the random initial population under the fixed GA parameters. Second, acoustic-model uncertainty may result from simplified classroom geometry, idealized boundary conditions, calibrated scattering coefficients, the simplified representation of desks and seats, and the assumptions of the ray-acoustics model. The comparison between simulated and measured post-renovation RT values showed an average absolute error of 0.04 s and an average relative error of 6.83%. The relative errors at 630 Hz and 2000 Hz were 15.56% and 12.50%, respectively, indicating greater model uncertainty at these frequency bands. Third, material-property uncertainty may arise from specimen variability and frequency-dependent differences in the sound absorption coefficients. Six specimens of each candidate material were tested, and the mean absorption coefficient at each frequency was used as the deterministic simulation input. However, specimen-to-specimen variability was not propagated through the optimization process and remains a limitation of the present uncertainty assessment. Fourth, construction-related uncertainty may arise from deviations in actual coverage area, panel joints, mounting conditions, installation positions, and differences between the idealized simulation layout and the implemented renovation. These uncertainty sources should be considered when the proposed framework is applied to other educational buildings.

4.3. Performance of Single-Material Acoustic Treatment Schemes

The effects of different acoustic materials on classroom RT and STI were evaluated using the simulation results. The comparison considered material absorption performance, effective frequency range, and feasible installation location. Figure 6 shows the simulated RT values for the nine single-material treatment schemes, while Figure 7 shows the corresponding STI values (Table 7).

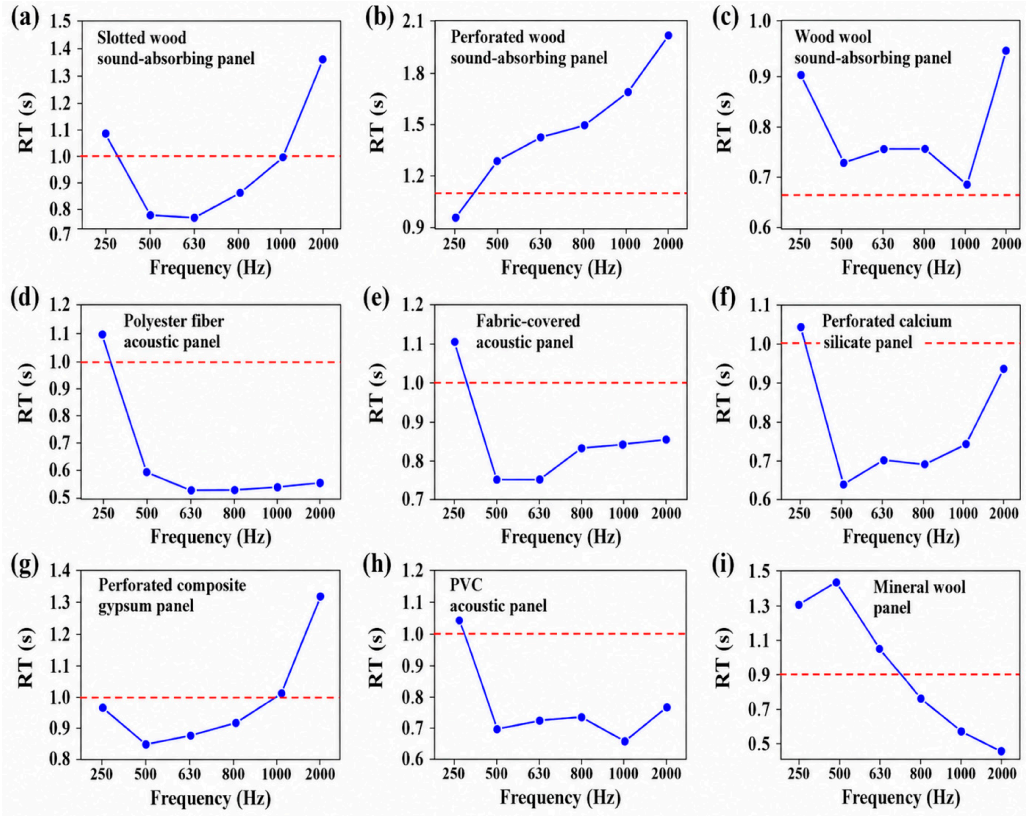


Figure 6. Simulated RT values under nine single-material acoustic treatment schemes. The dashed line indicates the standard limit of RT = 1.0 s.

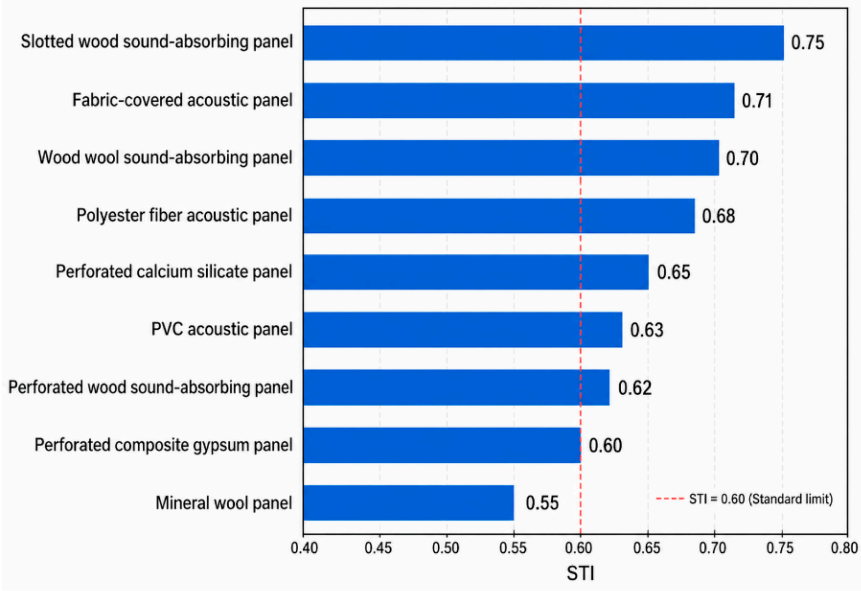


Figure 7. Simulated STI values under different single-material acoustic treatment schemes. The dashed line indicates the standard limit of STI = 0.60.

Table 7. Summary of simulated acoustic performance and interpretation under nine single-material treatment schemes.

Material	Main Effective Frequency Range	Representative RT Result	Main Acoustic Interpretation
Slotted wood sound-absorbing panel	Low frequency	RT at 250 Hz reduced from 2.42 s to 1.06 s	Slot resonance and backing cavity contributed to low-frequency reverberation control.
Perforated wood sound-absorbing panel	Mid frequency	RT in the 500–2000 Hz range reduced to 1.31–1.74 s	Perforated structure improved mid-frequency absorption but provided limited broadband control.
Wood wool sound-absorbing panel	Broadband mid-frequency absorption	RT values ranged from 0.69 s to 0.96 s	Porous and irregular fiber structure contributed to mid- and high-frequency absorption and sound scattering.
Polyester fiber acoustic panel	Mid- and high-frequency absorption	RT in the 500–2000 Hz range reduced to 0.55–0.59 s	High porosity improved mid- and high-frequency absorption.
Fabric-covered acoustic panel	Mid- and high-frequency absorption	RT in the 500–2000 Hz range reduced to 0.78–0.87 s	Fibrous structure enhanced sound absorption and scattering.
Perforated calcium silicate panel	Low- and mid-frequency absorption	RT in the 500–1000 Hz range reduced to 0.66–0.76 s	Perforation and rigid panel properties contributed to low- and mid-frequency control.
Perforated composite gypsum panel	Mid-frequency absorption	RT in the 500–2000 Hz range reduced to 0.88–1.32 s	Multilayer perforated structure provided moderate absorption but did not achieve balanced broadband control.
PVC acoustic panel	Mid-frequency absorption	RT in the 500–2000 Hz range reduced to 0.70–0.80 s	Microporous and flexible structure contributed to medium-frequency absorption.
Mineral wool panel	Mid- and high-frequency absorption	RT above 500 Hz showed clear reduction, with values ranging from 0.55 s to 1.44 s	Interconnected fibrous pores increased airflow resistivity and promoted viscous and thermal dissipation.

The single-material simulations showed that different materials had distinct frequency-dependent absorption characteristics. The slotted wood sound-absorbing panel was more effective for low-frequency reverberation control, reducing RT at 250 Hz from 2.42 s to 1.06 s. In contrast, porous and fibrous materials, such as polyester fiber acoustic panels, fabric-covered acoustic panels, and mineral wool panels, mainly improved mid- and high-frequency absorption. Wood wool sound-absorbing panels showed relatively balanced broadband performance, with RT values ranging from 0.69 s to 0.96 s. However, no single material simultaneously provided the best low-frequency control, broadband RT balance, STI improvement, and cost-effectiveness. Therefore, material-combination optimization was necessary to achieve balanced acoustic performance under the specified RT, STI, and cost constraints.

4.4. Performance of Optimized Material-Combination Schemes

The comprehensive performance of several material-combination schemes was further evaluated based on frequency-dependent absorption characteristics, installation location, RT reduction, and STI improvement. Figure 8 shows the simulated RT values before and after renovation under different material-combination schemes, while Figure 9 shows the corresponding STI results.

The combination of slotted wood sound-absorbing panel and mineral wool panel achieved the best overall acoustic performance. The slotted wood panel mainly improved low-frequency absorption, while the mineral wool panel contributed to mid- and high-frequency absorption. In the simulation results, this combination reduced RT from 2.42–1.76 s before renovation to 0.43–0.82 s after optimization and increased the simulation-based STI from 0.19 to 0.75, thereby satisfying the acoustic constraints. The combination of the perforated wood sound-absorbing panel and polyester fiber acoustic panel mainly improved mid- and high-frequency absorption. In the 500–2000 Hz range, RT decreased

from 1.99–1.74 s to 0.55–1.17 s, and STI reached 0.70. However, its low-frequency control was weaker than that of the slotted wood sound-absorbing panel and mineral wool panel combination.

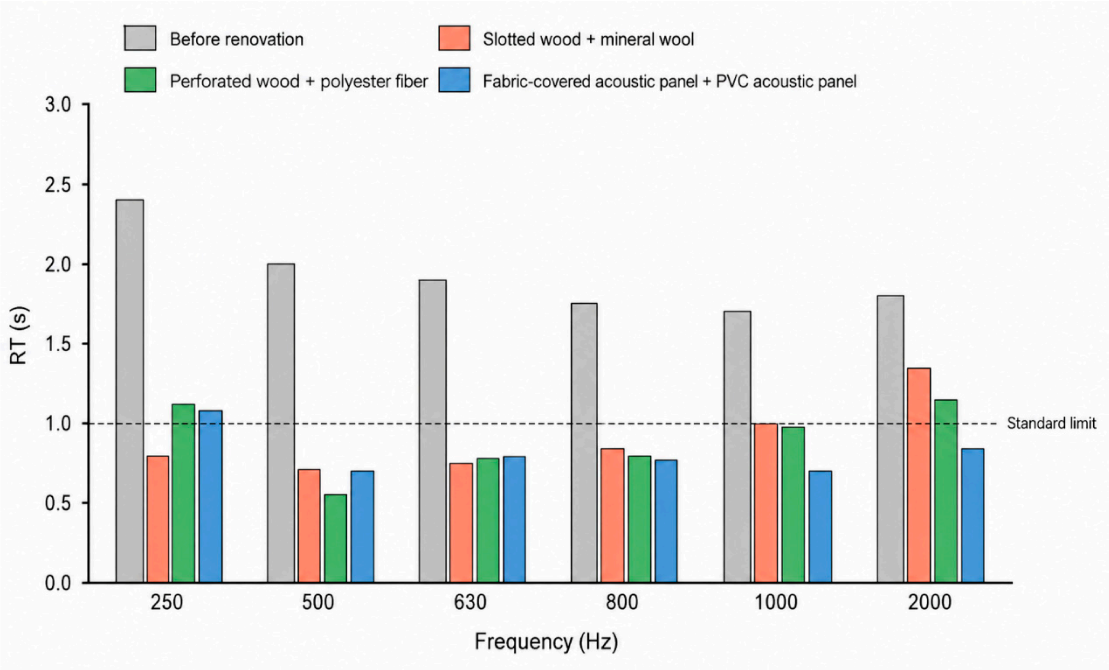


Figure 8. Simulated RT values before and after renovation under different material-combination schemes. The dashed line indicates the standard limit of RT = 1.0 s.

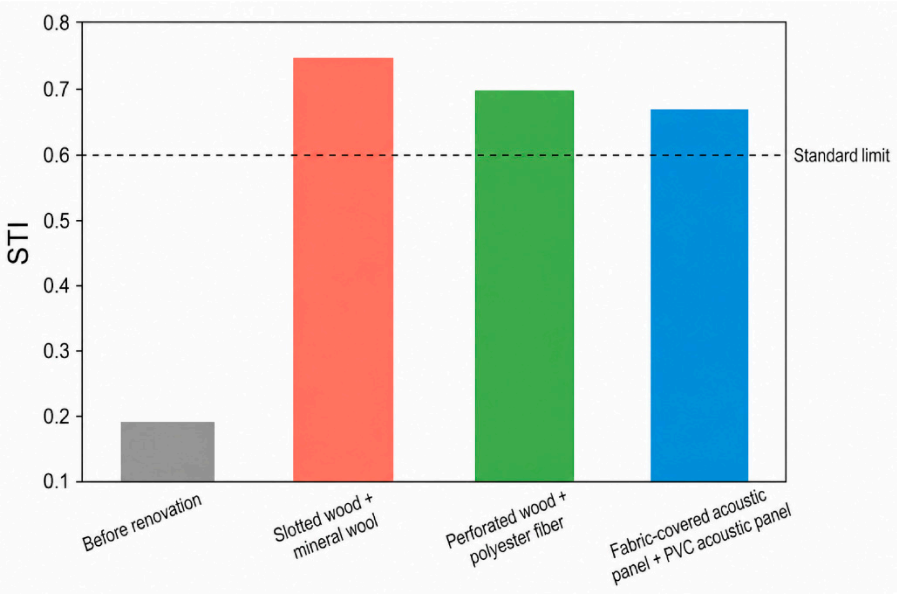


Figure 9. Simulated STI values before and after renovation under different material-combination schemes. The dashed line indicates the standard limit of STI = 0.60.

The combination of fabric-covered acoustic panel and PVC acoustic panel also improved mid-frequency absorption, reducing RT in the 500–2000 Hz range to 0.70–0.87 s, with an STI value of 0.67. The fabric-covered acoustic panel and PVC acoustic panel combination also improved speech-related frequency bands, but its constituent materials had relatively higher unit prices and its low-frequency absorption was less effective. Because

the optimized coverage areas were not calculated for this alternative, its total material cost cannot be directly compared with that of the selected configuration.

Although some combinations achieved lower RT values at specific frequencies, the optimal scheme should be evaluated based on broadband RT balance, STI improvement, compliance with acoustic constraints, material cost, installation feasibility, and acoustic-mechanism complementarity rather than the minimum RT at a single frequency. The perforated wood sound-absorbing panel and polyester fiber acoustic panel combination improved mid- and high-frequency absorption, but its low-frequency control was weaker. The fabric-covered acoustic panel and PVC acoustic panel combination also improved speech-related frequency bands, but its material cost was higher and its low-frequency absorption was less effective. In contrast, the slotted wood sound-absorbing panel and mineral wool panel combination provided complementary acoustic functions: the slotted wood panel contributed to low-frequency resonance absorption near the front-wall sound-source area, while the mineral wool ceiling treatment provided porous dissipation in the mid- and high-frequency ranges. This combination also satisfied the RT and STI constraints, maintained feasible installation on available classroom surfaces, and showed the lowest mean unit-price level among the three illustrative combinations; however, a direct total-cost comparison requires the actual coverage area of each material.

4.5. Cost-Effectiveness and Benchmark Comparison

In addition to acoustic performance, material cost was considered in the optimization process. The GA-identified configuration had a total material cost of 1512 RMB, calculated from the unit price and optimized coverage area of each selected material. Because the competing material combinations required different coverage areas to satisfy the acoustic constraints, simple arithmetic averages of their unit prices were not used as scheme-level cost indicators. A direct total-cost comparison between competing schemes requires the optimized coverage area and total material cost of each scheme.

To further clarify the advantage of the proposed optimization framework, the GA-based strategy was compared with conventional experience-based design and single-material selection strategies. Conventional experience-based acoustic renovation generally relies on designer judgment or company recommendations. Using interior material costing and design decision studies as contextual references, conventional experience-based renovation generally involves less transparent material-cost estimation than the proposed optimization-based framework [50–52]. In contrast, the proposed GA-based framework explicitly integrates material type, installation area, installation location, RT and STI constraints, and material cost into a unified optimization process (Table 8).

Table 8. Comparison between GA-based optimization and conventional design strategies.

Method	Material Selection Logic	Estimated Material Cost	RT Constraint	STI Constraint	Transparency
Conventional experience-based design	Based on designer experience or company recommendations	Generally higher and less transparent [50–52]	Not explicitly optimized	Not explicitly guaranteed	Low
Single-material treatment scheme	Based mainly on individual material absorption performance	Material-dependent	Frequency-dependent	May satisfy depending on material	Medium
Proposed GA-based framework	Constraint-based optimization of material type, coverage area, and installation location	1512 RMB in this case	Satisfied	Satisfied	High

Compared with conventional experience-based material selection, the proposed GA-based framework improves design transparency by explicitly defining the design variables, objective function, and acoustic constraints. Rather than selecting materials only according to individual absorption performance, the framework evaluates material type, coverage area, installation location, acoustic performance, and cost simultaneously. Therefore, within

the proposed acoustic constraint framework, the optimized solution satisfied the RT and STI requirements while providing a transparent and relatively low-material-cost solution for the classroom case considered in this study.

The cost model used in this study considered material cost as the primary economic objective. This choice was made to keep the optimization framework transparent and reproducible, because material unit prices and coverage areas can be directly linked to the material-layout variables. However, practical renovation decisions may also be influenced by installation cost, labor cost, maintenance cost, replacement frequency, durability, and end-of-life treatment. Including these additional cost components may change the final ranking of material schemes. For example, a material with a low unit price may become less favorable if it requires complex installation or frequent maintenance, whereas a material with a higher unit price may become more attractive if it offers better durability, easier construction, or lower life-cycle impact. Therefore, the proposed framework can be extended by replacing the current material-cost objective with a life-cycle cost or multi-criteria objective function in future applications.

Recent material-selection studies provide useful methodological references for such extensions. Ordu and Der developed a comparative hybrid MCDM approach for polymeric material selection in flexible pulsating heat pipe manufacturing [53]. Their decision model considered multiple material criteria and compared three hybrid methods, namely, AHP-GRA, AHP-CoCoSo, and AHP-VIKOR. The use of multiple ranking methods and rank-correlation analysis improved the transparency and robustness of material selection. Although their study focused on polymeric materials for thermal systems rather than acoustic renovation, the methodological logic is relevant to this study because acoustic material selection also involves multiple competing criteria, including acoustic performance, cost, installation feasibility, and environmental considerations.

Law and Narayan further emphasized that polymer material design should not only focus on material performance or biodegradability, but should also include feasible recovery and treatment pathways for managed end-of-life [54]. This perspective is important for future acoustic material selection because building renovation materials may differ in durability, recyclability, maintenance requirements, and disposal pathways. Inspired by these studies, future work will extend the current material-cost optimization model to a multi-criteria decision framework incorporating installation cost, maintenance demand, durability, environmental performance, and end-of-life management.

4.6. Field Validation of the Optimized Simulation-Based Design

After the optimized material configuration was obtained, the acoustic renovation scheme was implemented in the classroom. Mineral wool panels were installed on the ceiling with a total coverage area of 72 m^2, and slotted wood sound-absorbing panels were installed around the blackboard area on the front wall. The rear wall was left untreated. Field measurements were conducted using the same sound-source and receiver positions as those used in the calibrated COMSOL model.

In the field validation, the measured RT decreased from 2.42–1.76 s before renovation to 0.78–0.43 s after renovation. The difference between the simulated and measured post-renovation RT values was further analyzed to evaluate the predictive reliability of the calibrated model. These results confirmed that the optimized configuration satisfied the RT requirement in the field measurement, while the simulation-based STI evaluation predicted a potential improvement in speech intelligibility (Figures 10 and 11).



Figure 10. Classroom conditions: (**a**) before acoustic renovation and (**b**) after acoustic renovation.

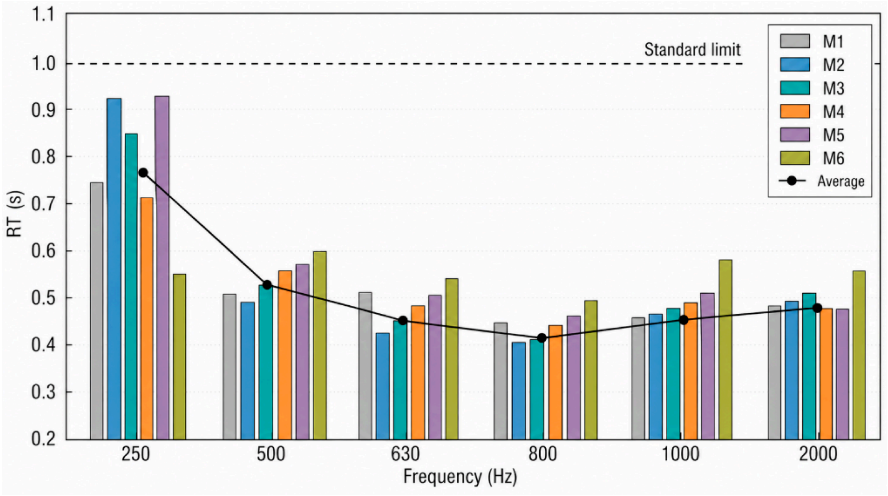


Figure 11. RT values at different receiver positions in the renovated classroom (M1–M6).

It should be noted that the field validation mainly focused on RT because RT was directly measured before and after renovation. STI was used as a simulation-based speech-intelligibility indicator in the optimization and performance evaluation. The simulated STI improvement should therefore be interpreted with caution. Its reliability is indirectly supported by the calibrated COMSOL model, which showed an average relative error of 6.83% between simulated and measured post-renovation RT values. Since reverberation decay and sound-energy distribution strongly affect speech intelligibility in the model, the RT validation provides partial support for the simulated STI trend. Nevertheless, the absence of direct field STI measurement remains a limitation of this study, and future work will include standardized STI measurements to further verify speech-transmission improvement. Although direct STI measurements were not available, the predicted post-renovation STI value of 0.75 was consistent with the improvement trend reported in previous classroom-acoustic studies using absorptive wall and ceiling treatments [29–32]. These studies showed that reducing excessive reverberation through absorptive treatments can improve speech intelligibility. Therefore, the simulated STI result in this study should be interpreted as a model-based prediction supported by RT validation and by consistency with previously reported classroom-acoustic improvement trends. The relative error between simulated and measured RT values was calculated to evaluate the reliability of the calibrated COMSOL model. As shown in Table 9, the absolute error between the simulated and measured RT values ranged from 0.01 s to 0.07 s, with an average absolute error of approximately 0.04 s. The average relative error was 6.83%, indicating that the calibrated simulation model could reasonably predict the acoustic performance of the classroom after material optimization. The relatively larger errors at 630 Hz and 2000 Hz may be related to simpli-

fied boundary conditions, uncertainty in scattering coefficients, and construction-related differences between the simulated and installed material layouts. Therefore, the COMSOL–MATLAB coupled optimization framework showed acceptable predictive reliability for supporting acoustic renovation decisions in educational buildings, as demonstrated by this classroom case.

Table 9. Comparison between simulated and measured RT values after acoustic renovation.

Frequency (Hz)	Simulated RT (s)	Measured RT (s)	Absolute Error (s)	Relative Error (%)
250	0.82	0.77	0.05	6.49
500	0.54	0.53	0.01	1.89
630	0.52	0.45	0.07	15.56
800	0.43	0.42	0.01	2.38
1000	0.45	0.46	0.01	2.17
2000	0.54	0.48	0.06	12.50
Average	—	—	0.04	6.83

4.7. Acoustic Mechanisms of the Optimized Configuration

The superior performance of the optimized configuration can be explained by four coupled mechanisms: resonance absorption, porous dissipation, frequency-band complementarity, and spatial material synergy.

The low-frequency improvement of the slotted wood sound-absorbing panel can be attributed to Helmholtz-type resonance absorption. The slot openings and backing cavity formed a resonant system, in which the air mass in the slots oscillated under incident sound excitation and dissipated acoustic energy through viscous and thermal losses. This mechanism is consistent with the observed reduction in RT at 250 Hz from 2.42 s to 1.06 s in the single-material scheme.

In contrast, the absorption behavior of the mineral wool panel was primarily governed by porous dissipation. The interconnected fibrous network increases airflow resistivity and promotes viscous friction and thermal exchange when sound waves propagate through the pores. This mechanism explains the improved absorption in the 500–2000 Hz range and contributes to the simulation-based increase in STI from 0.19 to 0.75 after optimization.

The combined use of the slotted wood sound-absorbing panel and mineral wool panel produced a frequency-band complementary effect. The slotted wood sound-absorbing panel mainly controlled low-frequency reverberation through resonance absorption, whereas the mineral wool panel attenuated mid- and high-frequency components through porous dissipation. This complementarity broadened the effective absorption range and contributed to the measured reduction in RT from 2.42–1.76 s to 0.78–0.43 s, as well as the simulation-based improvement of STI from 0.19 to 0.75.

Moreover, the spatial distribution of the two materials contributed to spatial material synergy. Installing mineral wool panels on the ceiling reduced repeated vertical reflections between the floor and ceiling, thereby suppressing the accumulation of reverberant energy in the mid- and high-frequency ranges. Meanwhile, the slotted wood sound-absorbing panels located around the blackboard area modified early reflection paths near the teacher's sound source, improving the balance between direct sound and reflected sound received by listeners. This spatial redistribution of acoustic functions contributed to the superior broadband performance of the optimized hybrid configuration and explains why it achieved better broadband RT control and simulation-based STI improvement than single-material schemes. The optimized design therefore works through a coupled material–frequency–space mechanism: the slotted wood panel controlled low-frequency reflections near the sound source, while the mineral wool ceiling treatment attenuated mid- and high-frequency

reverberation over a larger surface area. This combined mechanism improved broadband RT balance and was associated with an increase in the simulation-based STI, suggesting a potential improvement in speech intelligibility.

Overall, the acoustic improvement achieved by the optimized design did not result from a single material property, but from the combined effects of resonance absorption, porous dissipation, frequency-band complementarity, and spatial material synergy. These mechanisms explain how the hybrid acoustic configuration combining wood-based resonant panels and porous absorptive materials improved acoustic performance while supporting cost-effective acoustic renovation of educational buildings in this classroom case.

4.8. Generalizability and Limitations

The proposed framework was demonstrated and field-validated using one unoccupied rectangular classroom. Therefore, the optimized material configuration and the associated numerical results should be interpreted as case-specific. Educational spaces may differ in room volume, geometry, ceiling height, glazing area, seating density, surface finishes, occupancy condition, and background-noise level. These differences may affect sound propagation, RT, STI, and the feasible installation areas of acoustic materials. Accordingly, the material layout obtained in the present case should not be directly transferred to another classroom without room-specific modeling and calibration.

Nevertheless, the modular structure of the proposed framework provides a methodological basis for adaptation to other educational spaces. For another application, the room geometry, boundary and material acoustic properties, source–receiver configuration, occupancy and background-noise assumptions, candidate material database, material prices, acoustic constraints, and constructability limits should be updated. The acoustic model should then be recalibrated before the optimization procedure is repeated. This methodological adaptability should not be interpreted as empirical validation of external transferability, which remains to be examined using additional classroom cases.

Several limitations remain. First, STI was evaluated through simulation rather than direct field measurement. The measured RT results provide validation of the modeled reverberation-decay behavior but do not constitute direct experimental validation of the absolute STI values. Second, the economic objective considered material cost only and excluded installation, labor, maintenance, replacement, and life-cycle costs. Third, the study was conducted under the Chinese classroom-acoustic standard system. Application under relevant European or international standards would require the remeasurement or appropriate conversion of material acoustic properties, reconstruction of the candidate material database, redefinition of the acoustic performance constraints, re-execution of the optimization procedure, and additional field validation. Therefore, the framework has not yet been empirically validated under European regulatory requirements, and a complete European-standard reanalysis would require additional material characterization, optimization, and field measurements.

The three independent GA runs used different random initial populations but identical population size, crossover rate, mutation rate, and generation limit. Therefore, these runs evaluate repeatability with respect to initial-population randomness only and do not establish that the optimization result is insensitive to GA parameter settings. Future studies should validate the framework in educational spaces governed by different regulatory requirements and examine how variations in acoustic standards affect the material database, performance constraints, optimization results, and field-validation procedures. Direct field STI measurement, systematic GA parameter-sensitivity analysis, and an extended life-cycle cost model should also be incorporated.

4.9. Comparison with Previous Acoustic Renovation Studies for Educational Spaces

Compared with previous acoustic renovation studies for classrooms and educational buildings that mainly relied on empirical material placement or post-design acoustic simulation, the proposed framework explicitly integrates material type, coverage area, installation location, RT and STI constraints, and material cost into a unified optimization process. Previous studies have demonstrated that wall and ceiling absorptive treatments can effectively reduce RT and improve speech intelligibility. However, the selection of material combinations and coverage areas is often determined by designer experience or by comparing a limited number of predefined schemes. In contrast, the present framework treats acoustic renovation as a constrained building performance optimization problem. This allows the optimized solution to satisfy acoustic requirements while maintaining a relatively low material cost. Therefore, the main contribution of this study lies not only in the improvement of acoustic indicators in the classroom case, but also in providing a transparent and reproducible decision-support workflow for the cost-effective renovation of educational buildings. Unlike studies that only report the acoustic effect of a predefined treatment scheme, the present framework links material selection, coverage area, installation location, cost minimization, and field validation within a single optimization process.

4.10. Design Implications

Based on the results of the present classroom case, three design implications can be identified for the acoustic renovation of educational spaces. First, acoustic materials should be selected according to their effective absorption frequency ranges. Resonant wood-based panels may contribute to low-frequency reverberation control, whereas porous materials such as mineral wool panels can provide effective absorption in the mid- and high-frequency ranges. Second, acoustic treatments should be prioritized on acoustically influential reflection surfaces. In the present case, the ceiling treatment reduced the accumulation of reverberant energy over a relatively large surface area, while the front-wall treatment acted near the teacher's sound-source position. Third, material type, coverage area, and installation location should be considered jointly rather than independently. A coordinated layout can improve broadband RT control while avoiding excessive concentration of absorptive treatment and unnecessary material use.

5. Conclusions

This study developed a COMSOL–MATLAB coupled simulation–optimization framework for cost-effective acoustic renovation of existing educational buildings, using a real classroom as the validation case. The framework integrated acoustic prediction, GA-based material-layout optimization, material cost minimization, constructability constraints, and field validation. By treating material type, coverage area, and installation location as decision variables, the proposed workflow provides a quantitative decision-support method for the acoustic renovation of educational buildings.

The optimized configuration consisted of slotted wood sound-absorbing panels installed around the blackboard area and mineral wool panels installed on the ceiling. Field measurements showed that RT decreased from 2.42–1.76 s before renovation to 0.78–0.43 s after renovation. The simulation-based STI evaluation indicated improved speech intelligibility, with STI increasing from 0.19 to 0.75. The total material cost was 1512 RMB, indicating that the proposed framework can improve acoustic performance while supporting cost-controlled renovation under project-specific material prices and constraints. The average relative error between simulated and measured RT values was 6.83%, supporting the predictive reliability of the calibrated acoustic model.

Mechanism analysis indicated that the acoustic improvement resulted from the combined effects of resonance absorption, porous dissipation, frequency-band complementarity, and spatial material synergy. These findings suggest that hybrid acoustic configurations combining wood-based resonant panels and porous absorptive materials can support the acoustic renovation of educational buildings by improving broadband RT control and speech intelligibility while maintaining reasonable material cost.

The present study was validated using a single classroom case. Future studies should apply the framework to classrooms with different geometries, occupancy conditions, and background noise levels. Additional runs under varied GA parameter settings and additional classroom models are needed to evaluate robustness beyond the three initial-population runs reported in this study.

Author Contributions: S.Y. contributed to conceptualization, methodology, data curation, and writing—original draft. Y.M. contributed to supervision and software. L.Z. and Z.L. contributed to conceptualization. All authors have read and agreed to the published version of the manuscript.

Funding: This study was financially supported by the National Natural Science Foundation of China (grant no. 32271781).

Data Availability Statement: The data that support the findings of this study are available from the corresponding author upon reasonable request.

Conflicts of Interest: The authors declare no conflicts of interest.

References

1. Yan, S.; Zhang, L.; Miao, Y.; Deng, J.; Liu, Z. Research on regulating classroom Reverberation Time by using wood materials. *J. Build. Eng.* **2025**, *103*, 112173. [CrossRef]
2. Yan, S.; Zhang, L.; Zhang, L.; Qi, F.; Liu, Z. Research progress on indoor acoustic regulation using wood materials. *For. Prod. Ind.* **2019**, *61*, 48–53.
3. Ryan, S.; Mendel, L.L. Acoustics in physical education settings: The learning roadblock. *Phys. Educ. Sport Pedagog.* **2010**, *15*, 71–83. [CrossRef]
4. Zannin, P.H.T.; Loro, C.P. Measurement of the ambient noise level, reverberation time and transmission loss for classrooms in a public school. *Noise Control Eng. J.* **2007**, *55*, 327–333. [CrossRef]
5. Mogas-Recalde, J.; Palau, R.; Márquez, M. How classroom acoustics influence students and teachers: A systematic literature review. *J. Technol. Sci. Educ.* **2021**, *11*, 245–259. [CrossRef]
6. Shield, B.; Conetta, R.; Dockrell, J.; Connolly, D.; Cox, T.; Mydlarz, C. A survey of acoustic conditions and noise levels in secondary school classrooms in England. *J. Acoust. Soc. Am.* **2015**, *137*, 177–188. [CrossRef] [PubMed]
7. Sarlati, S.; Haron, Z.; Yahya, K.; Darus, N.; Dimon, N.; Athari, P. The importance of acoustic quality in classroom. *J. Teknol.* **2014**, *70*, 71–76. [CrossRef]
8. Chen, Q.; Ou, D. The effects of classroom reverberation time and traffic noise on English listening comprehension of Chinese university students. *Appl. Acoust.* **2021**, *179*, 108082. [CrossRef]
9. Liu, C.; Zang, Q.; Li, J.; Pan, X.; Dai, H.; Gao, W. The effect of the acoustic environment of learning spaces on students' learning efficiency: A review. *J. Build. Eng.* **2023**, *79*, 107911. [CrossRef]
10. Rosenberg, G.G. Classroom acoustics. *Semin. Hear.* **2010**, *31*, 188–202. [CrossRef]
11. Rabelo, A.T.V.; Santos, J.N.; Oliveira, R.C.; Magalhães, M.C.; Carvalho, S.A. Effect of classroom acoustics on the speech intelligibility of students. *CoDAS* **2014**, *26*, 360–366. [CrossRef] [PubMed]
12. Bistafa, S.R.; Bradley, J.S. Reverberation time and maximum background-noise level for classrooms from a comparative study of speech intelligibility metrics. *J. Acoust. Soc. Am.* **2000**, *107*, 861–875. [CrossRef] [PubMed]
13. Jaramillo, A.M.; Olson, B.C.; Nelson, P.; Bochat, S.; Doing, M. *Qualitative Evaluation of a Classroom Redesign*; Universitatsbibliothek der RWTH Aachen: Aachen, Germany, 2019.
14. Berg, F.S.; Blair, J.C.; Benson, P.V. Classroom acoustics: The problem, impact, and solution. *Lang. Speech Hear. Serv. Sch.* **1996**, *27*, 16–20. [CrossRef]
15. Nijs, L.; Rychtarikova, M. Calculating the optimum Reverberation Time and absorption coefficient for good speech intelligibility in classroom design using U50. *Acta Acust. United Acust.* **2011**, *97*, 93–102. [CrossRef]

16. Lombardo, A. *Classroom Acoustics Design: Algorithms to Optimize Typology, Extension and Position of Acoustic Materials to Improve Teaching-Learning Activities*; Politecnico di Torino: Torino, Italy, 2019.
17. Yan, S.; Zhang, L.; Liu, Z.; Wang, H. Acoustic Optimization of Classroom Environments Using Oriented Strand Board Panels: Layout Strategy and Simulation Validation. *Buildings* **2026**, *16*, 2159. [CrossRef]
18. Tao, Y.; Ren, M.; Zhang, H.; Peijs, T. Recent progress in acoustic materials and noise control strategies—A review. *Appl. Mater. Today* **2021**, *24*, 101141. [CrossRef]
19. Cowan, J. Building acoustics. In *Springer Handbook of Acoustics*; Springer: Berlin/Heidelberg, Germany, 2014; pp. 403–442.
20. Seddeq, H.S. Factors influencing acoustic performance of sound absorptive materials. *Aust. J. Basic Appl. Sci.* **2009**, *3*, 4610–4617.
21. Bucur, V. *The Acoustics of Wood (1995)*; CRC Press: Boca Raton, FL, USA, 2017.
22. Liu, Z.; Li, X.; Yu, Y.; Wan, K.; Hao, Q.; Wang, Y.; Wang, C. Effects of wood powder and compatibilizer content on acoustic vibration properties of wood-plastic composites. *For. Eng.* **2022**, *38*, 62–67.
23. Asdrubali, F.; Ferracuti, B.; Lombardi, L.; Guattari, C.; Evangelisti, L.; Grazieschi, G. A review of structural, thermo-physical, acoustical, and environmental properties of wooden materials for building applications. *Build. Environ.* **2017**, *114*, 307–332. [CrossRef]
24. Bucur, V. Wood and Wood-Based Materials in Architectural Acoustics. In *Acoustics of Wood*; Springer Series in Wood Science; Springer: Berlin/Heidelberg, Germany, 2006; pp. 21–36.
25. Alapieti, T.; Mikkola, R.; Pasanen, P.; Salonen, H. The influence of wooden interior materials on indoor environment: A review. *Eur. J. Wood Wood Prod.* **2020**, *78*, 617–634. [CrossRef]
26. Liu, Z.; Shen, J. *Vibration Characteristics of Soundboard Materials and Acoustic Quality of Piano*; Science Press: Beijing, China, 2009.
27. Xu, D.; Hao, J.; Jiang, H.; Wu, X.; Zhu, X. Research on sound insulation performance of lightweight composite wood door based on vertical corrugated structure. *J. For. Eng.* **2024**, *9*, 48–54.
28. Wu, Y.; Wang, Y.T.; Huang, Z.L.; Lin, Y.F.; Li, H.M.; Wang, Z.Q.; Zhu, Y.X. Effect of recombination bamboo square pin on mechanical and acoustic properties of orthogonal glulam. *J. For. Eng.* **2024**, *9*, 152–159.
29. Iannace, G.; Maffei, L.; Trematerra, P. On the use of "green materials" for the acoustic renovation of classrooms. In Proceedings of the EURONOISE, Prague, Czech Republic, 10–13 June 2012; pp. 89–94.
30. Selim, A.M.; Saeed, D.M. Enhancing the classroom acoustic environment in Badr University, Egypt: A case study. *Build. Acoust.* **2022**, *29*, 577–596. [CrossRef]
31. Torabia, M.R.; Loghmanib, A. Acoustical simulation, design and experimental investigation of a classroom: A case study. *J. Theor. Appl. Vib. Acoust.* **2021**, *9*, 1–20.
32. Russo, D.; Ruggiero, A. Choice of the optimal acoustic design of a school classroom and experimental verification. *Appl. Acoust.* **2019**, *146*, 280–287. [CrossRef]
33. Labia, L.; Shtrepi, L.; Astolfi, A. Improved room acoustics quality in meeting rooms: Investigation on the optimal configurations of sound-absorptive and sound-diffusive panels. *Acoustics* **2020**, *2*, 451–473.
34. Mir, S.H.; Abdou, A.A. Investigation of sound-absorbing material configuration of a smart classroom utilizing computer modeling. *Build. Acoust.* **2005**, *12*, 175–188. [CrossRef]
35. Ribeiro, R.S.; Amlani, A.M.; de Conto, J.; Schwerz, B.G.; Amarilla, R.S.D.; Sant'aNa, L.H.; Avelar, M.; Catai, R.E.; Matoski, A. Acoustical treatment characterization of a classroom with wood-based composites. *Appl. Acoust.* **2021**, *178*, 107967. [CrossRef]
36. *IEC 60268-16:2020*; Sound System Equipment—Part 16: Objective Rating of Speech Intelligibility by Speech Transmission Index. International Electrotechnical Commission: Geneva, Switzerland, 2020.
37. Klein, W. Articulation Loss of Consonants as a Basis for the Design and Judgement of Sound Reinforcement Systems. *Audio Eng. Soc.* **1971**, *19*, 920–925.
38. Ballou, G. *Handbook for Sound Engineers*; Taylor & Francis: Abingdon, UK, 2013.
39. Puglisi, G.E.; Warzybok, A.; Astolfi, A.; Kollmeier, B. Effect of reverberation and noise type on speech intelligibility in real complex acoustic scenarios. *Build. Environ.* **2021**, *204*, 108137. [CrossRef]
40. *GBJ 88-1985*; Specification for Measurement of Sound Absorption Coefficient and Acoustic Impedance by Standing Wave Tube Method. Standardization Administration of China: Beijing, China, 1985.
41. *GB/T 18696.1-2004*; Acoustics—Measurement of Acoustic Impedance in Impedance Tubes—Part 1: Standing Wave Ratio Method. Standardization Administration of China: Beijing, China, 2004.
42. *GB 50118-2010*; Code for Sound Insulation Design of Civil Buildings. Ministry of Housing and Urban-Rural Development of the People's Republic of China: Beijing, China, 2010.
43. Liu, X. *Building Physics*, 2nd ed.; China Building Industry Press: Beijing, China, 2000.
44. *GB/T 36075.2-2018*; Acoustics—Measurement of Room Acoustic Parameters—Part 2: Reverberation Time in Ordinary Rooms. Standardization Administration of China: Beijing, China, 2018.
45. Dalenback, B.I.; Brown, S. Characterizing rooms regarding Reverberation Time prediction and the sensitivity to absorption and scattering coefficient accuracy. *J. Acoust. Soc. Am.* **2010**, *127*, 1752. [CrossRef]

46. Vorländer, M. International round robin on room acoustical computer simulations. In Proceedings of the 15th International Congress on Acoustics, Trondheim, Norway, 26–30 June 1995.
47. Christensen, C.L.; Rindel, J.H. A new scattering method that combines roughness and diffraction effects. In Proceedings of the Forum Acousticum, Budapest, Hungary, 29 August–2 September 2005; pp. 344–352.
48. Bistafa, S.R.; Bradley, J.S. Predicting Reverberation Times in a simulated classroom. *J. Acoust. Soc. Am.* **2000**, *108*, 1721–1731. [CrossRef] [PubMed]
49. Saraswat, M.; Sharma, A.K. Genetic Algorithm for optimization using MATLAB. *Int. J. Adv. Res. Comput. Sci.* **2013**, *4*, 155–159.
50. Moussatche, H.; Languel, J. Life cycle costing of interior materials for Florida's schools. *J. Inter. Des.* **2002**, *28*, 37–49. [CrossRef]
51. Allison, D. *Estimating and Costing for Interior Designers: A Step-By-Step Workbook*; A&C Black: London, UK, 2014.
52. Lee, H.; Lee, Y.; Kim, J. A cost-based interior design decision support system for large-scale housing projects. In *Convergence and Hybrid Information Technologies*; IntechOpen: London, UK, 2010.
53. Ordu, M.; Der, O. Polymeric Materials Selection for Flexible Pulsating Heat Pipe Manufacturing Using a Comparative Hybrid MCDM Approach. *Polymers* **2023**, *15*, 2933. [CrossRef] [PubMed]
54. Law, K.L.; Narayan, R. Reducing Environmental Plastic Pollution by Designing Polymer Materials for Managed End-of-Life. *Nat. Rev. Mater.* **2022**, *7*, 104–116.

Disclaimer/Publisher's Note: The statements, opinions and data contained in all publications are solely those of the individual author(s) and contributor(s) and not of MDPI and/or the editor(s). MDPI and/or the editor(s) disclaim responsibility for any injury to people or property resulting from any ideas, methods, instructions or products referred to in the content.